

# An Investigation of Optimized Length Scales of the Heat Treatment of Metallic Plates

A. ALI and K. VAFAI

Department of Mechanical Engineering, Ohio State University, Columbus, Ohio, USA

*A moving metallic plate subject to heating and cooling boundary conditions is considered in this work. The plate is heated by an imposed heat flux, and cooled down by an array of impinging jets through convection and radiation. The objective of the present work is determination of operating conditions for controlling the temperature distribution at the end of both heating and cooling sections. The results show that the temperature distribution becomes more uniform across the heating section with an increase in the heating length. An increase in the distance from the impinging jet to the plate causes an increase in the temperature values across the cooling section, and a decrease in the diameter of the impinging jet causes a decrease in the temperature values across the cooling section. It is also shown that an increase in cooling length and the addition of another impinging jet help to reduce the temperature values and increase the uniformity of the structure across the cooling section. Optimized values of the pertinent parameters for both hardening and tempering heat treatments were investigated.*

Heat treatment of metals is used to improve the mechanical properties of metals in their solid-state phase [1]. Heat treatment is employed to achieve desired metal designs in aircraft, automobile industries, and other branches of engineering [2]. In the past few decades, numerical simulation has received considerable attention because it predicts the thermal response of a moving plate or cylinder that is subjected to different kinds of boundary conditions. The applications of heated moving surfaces are not limited to heat treatments, but also extend to hot rolling, wire drawing, extrusion, continuous casting, and crystal growing processes [3].

Address correspondences to Dr. K. Vafai, Mechanical Engineering Department, Ohio State University, 1067 Robinson Laboratory, 206 W. Eighteenth Ave., Columbus, OH 43210, USA. E-mail: vafai.1@osu.edu

Various studies have been performed to investigate the thermal response of heated moving surfaces in the past few decades. Jaluria and Singh [4] numerically investigated both the transient and steady-state cases for heated materials, which move at a constant velocity. For a two-dimensional unsteady heat conduction equation, their numerical results were obtained using a Crank-Nicolson implicit formulation along with Guess-Sidel iterative method. Their results showed that the isotherms were almost parallel to the radial direction for low values of Biot numbers. In addition, their results showed that isotherms became more convex, which indicated the temperature decay at the surface and gradual decay at the centerline for high values of Biot number. Karwe and Jaluria [5] studied the effects of a heated moving plate that involved a conjugate heat transfer investigation. Their results indicated that the transverse



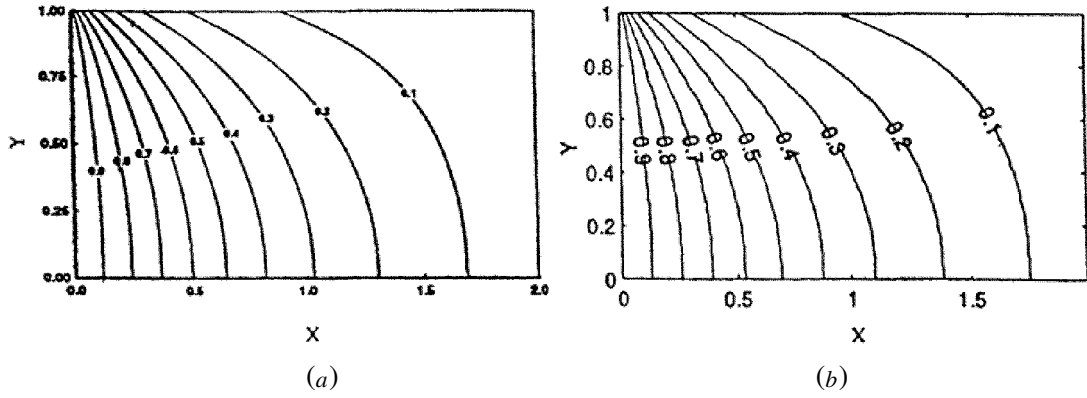


**Figure 3** Comparison between (a) analytical [14] and (b) numerical dimensionless temperature distribution solutions, where  $\kappa = 10.0$ ,  $Pe = 0.2$ ,  $Bi = 5.0$ .

increase in the plate speed caused a decrease in the total heat transfer. Also, a decrease in the nozzle height caused an increase in the average heat transfer rate. Taga et al. [10] experimentally investigated the cooling of a

hot moving plate by impinging water jets. Their results indicated that an increase in the plate speed, while keeping the initial temperature of the plate at low values, caused an increase in the average heat flux.

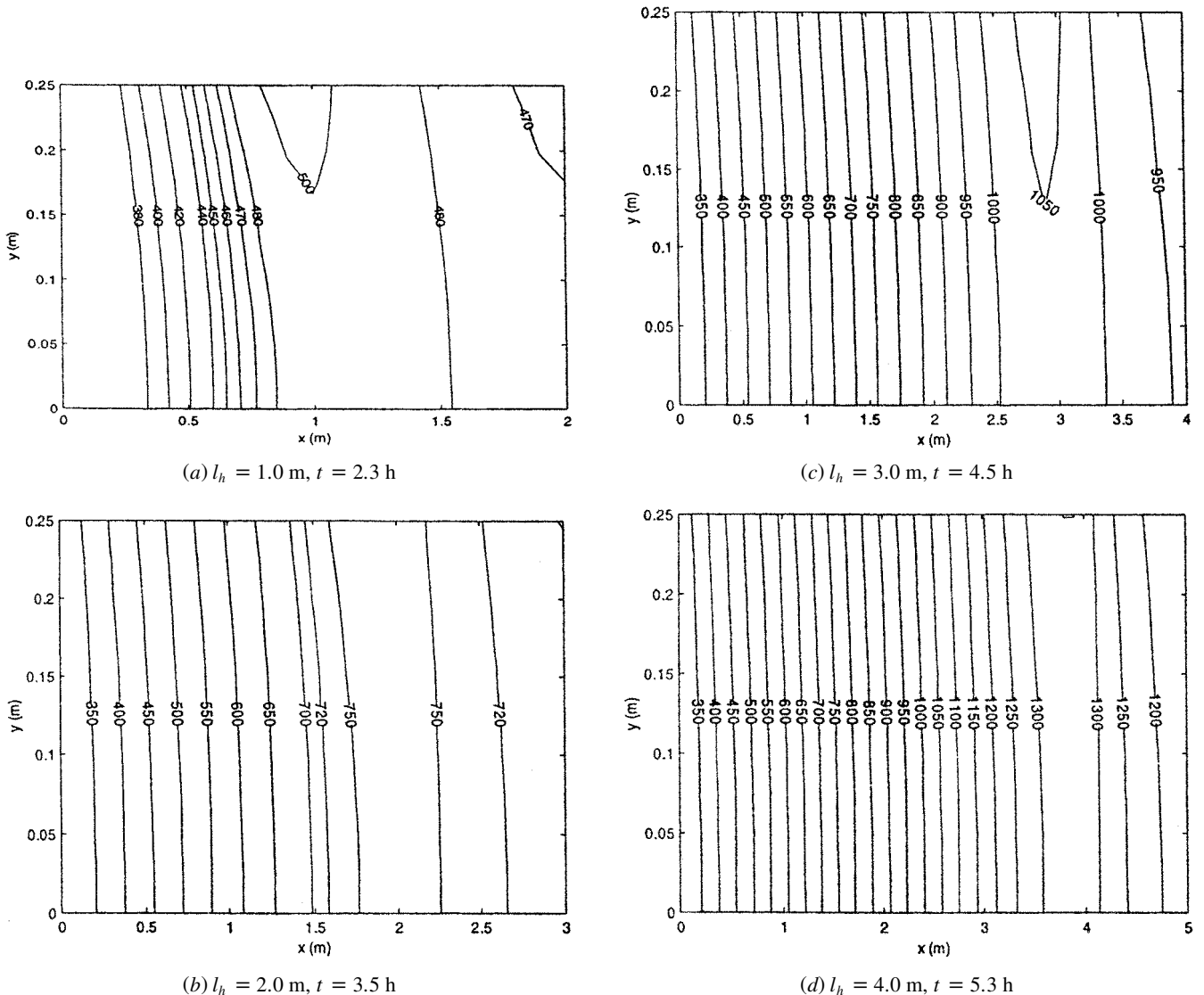


**Figure 4** Steady-state temperature distribution throughout the plate for different heating lengths, where  $K = 1.0$ ,  $l_{c1} = 1.0$  m,  $l_g = 50,000 \frac{w}{m^2}$ ,  $\frac{w_l}{d_n} = 2.5$ ,  $\frac{s_{np1}}{d_n} = 2.0$ ,  $Re_i = 114,000$ ,  $Pe = 0.712$ .

Recently, Lee and Vafai [11] investigated impinging jet and microchannel cooling for high-heat-flux applications. Single and multiple impinging jets were analyzed with different shapes of nozzles. The impinging jet was better than microchannel cooling for a larger plate when the spent flow was properly treated and applied after the impinging jet. The results from their work will be used in the present investigation.

Most studies have considered either heating or cooling conditions associated with moving materials. In the present study, a combination of both heating and cooling boundary conditions is imposed on a moving plate and the thermal response of the moving metallic plate is investigated. The objective of the present work is to examine the control of the temperature of the plate at the end of both heating and cooling sections, and optimization of both heating and cooling lengths. Another objective is to investigate conditions under which one can maintain the temperature distribution across the thickness of a metallic plate as uniformly as possible in order to keep uniformity of the structure. For example, if a steel metal is heated beyond a critical range, a uniform structure cannot be obtained. The effect of various parameters in achieving a uniform temperature distribution is discussed in this investigation. The pertinent parameters are heating and cooling lengths, speed of the plate, speed of the coolant fluid, distance from the plate to the impinging jet, and the diameter of the impinging jet. The optimization of the controlling parameters in the heat treatment processes is also discussed.

**PROBLEM FORMULATION**

A metal plate moving at a constant speed,  $u_p$ , is considered, as shown in Figure 1. The setup shown in Figure 1 displays only the upper half of the plate ( $0 \leq y \leq b$ ), because of symmetry. In the heating section a constant heat flux is imposed, and in the cooling section an array of impinging jets is utilized.

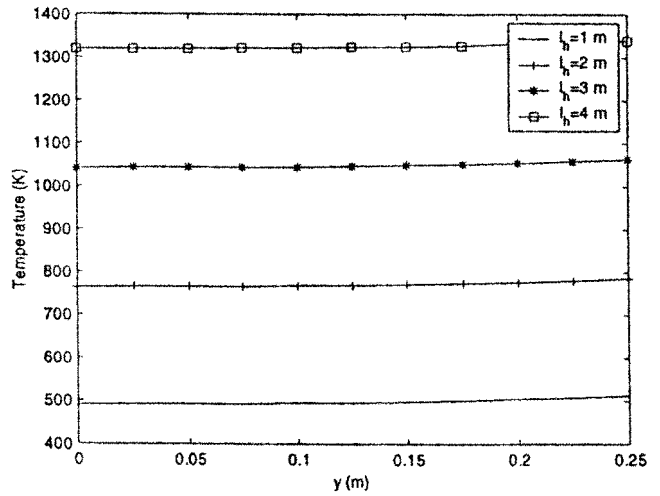
The two-dimensional unsteady heat conduction equation is considered for the plate while accounting for the plate movement.

$$\frac{\partial T}{\partial t} + u_p \frac{\partial T}{\partial x} = \alpha \left( \frac{\partial^2 T}{\partial x^2} + \frac{\partial^2 T}{\partial y^2} \right) \quad (1)$$

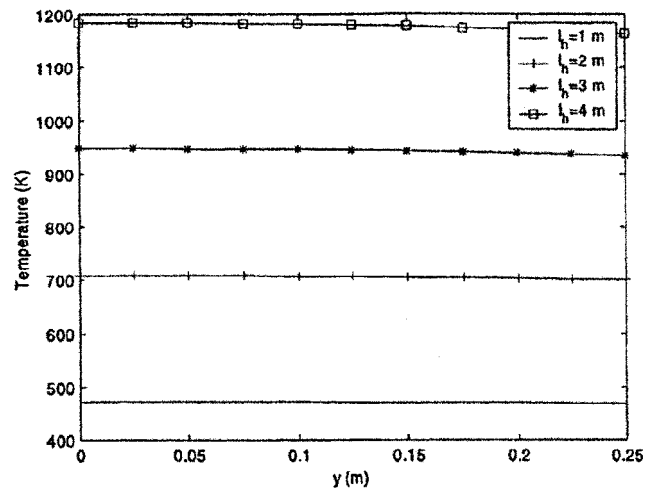
It is necessary to include the transient term in Eq. (1) in order to account for the time it takes to reach the steady-state solution for both heating and cooling sections. Due to the motion of the plate in the axial direction, it is necessary to account for convective terms. Both terms are necessary for designing the system.

The initial condition and boundary conditions are

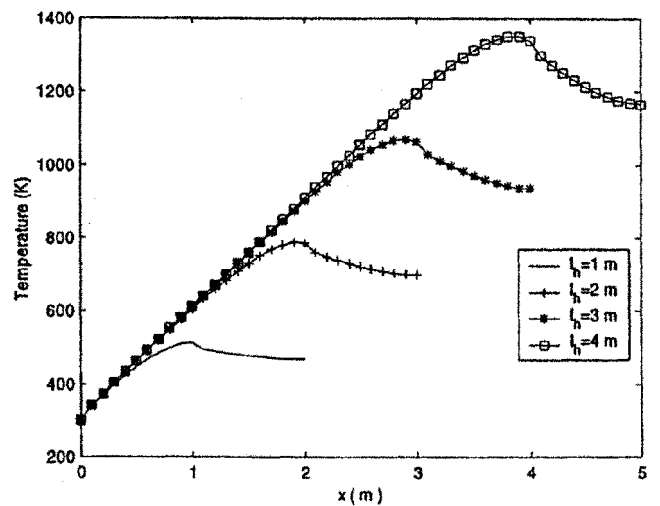
$$T = T_i \quad \text{at } t = 0 \quad (2)$$



(a)



(b)



(c)

**Figure 5** (a) Transverse temperature distribution at the end of the heating section, (b) transverse temperature distribution at the end of the cooling section, and (c) axial temperature distribution at the top surface, for different heating lengths.

## IMPINGING JET ANALYSIS

It is important to analyze the impinging jet in order to determine the average heat transfer coefficient,  $h_j$ , across the impinging jet. Based on Lee and Vafai's [11] and Martin's [12] works, the Nusselt number for the present impinging jet arrangement can be written as

$$\frac{Nu}{Pr^{0.42}} = G\left(\frac{d_j}{w_j}, \frac{S_{npj}}{d_j}\right) FF(Re_j) \quad (9)$$

where

$$G\left(\frac{d_j}{w_j}, \frac{S_{npj}}{d_j}\right) = \frac{d_j}{w_j} \frac{1 - 1.1(d_j/w_j)}{1 + 0.1[(S_{npj}/d_j) - 6](d_j/w_j)} \quad (10)$$

$$\frac{\partial T}{\partial y} = 0 \quad \text{at } 0 \leq x < l_h \text{ and } y = 0 \quad (3)$$

$$k_p \frac{\partial T}{\partial y} = q_s \quad \text{at } 0 \leq x < l_h \text{ and } y = b \quad (4)$$

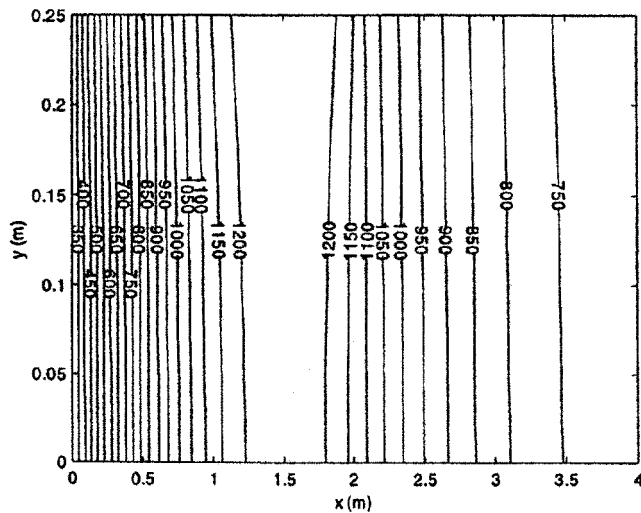
$$T = T_{ENT} \quad \text{at } x = 0 \text{ and } 0 \leq y \leq b \quad (5)$$

$$\frac{\partial T}{\partial y} = 0 \quad \text{at } l_h \leq x \leq l_{cj} \text{ and } y = 0 \quad (6)$$

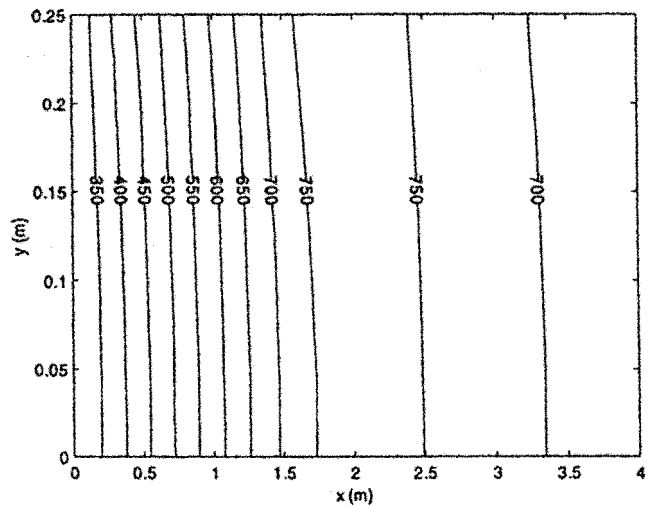
$$-k_p \frac{\partial T}{\partial y} = \varepsilon \sigma F(T^4 - T_e^4) + h_j(T - T_w) \quad (7)$$

at  $l_h \leq x \leq l_{cj}$  and  $y = b$

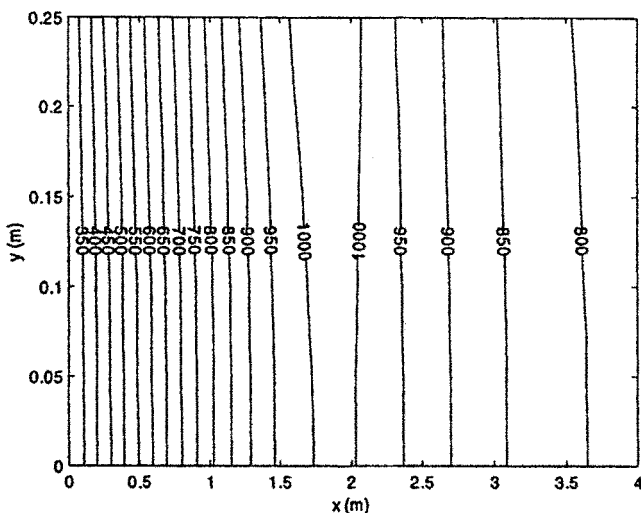
$$\frac{\partial T}{\partial x} = 0 \quad \text{at } x = l_h + \sum_{j=1}^K l_{cj} \text{ and } 0 \leq y \leq b \quad (8)$$



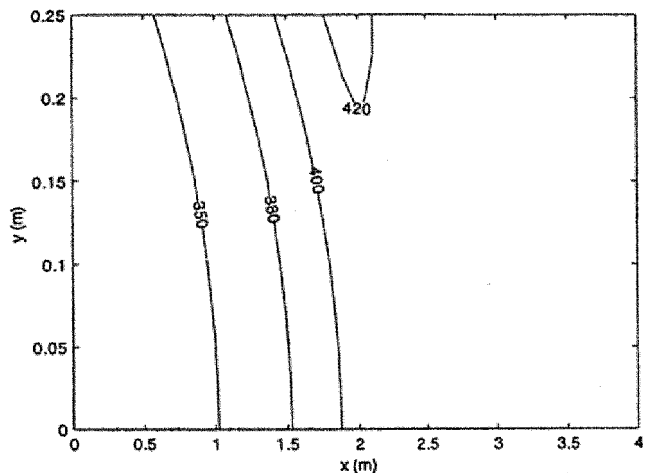
(a)  $Pe = 0.0712, t = 14.148 \text{ h}$



(c)  $Pe = 0.712, t = 4.278 \text{ h}$



(b)  $Pe = 0.356, t = 7.986 \text{ h}$



(d)  $Pe = 3.56, t = 0.638 \text{ h}$

**Figure 6** Steady-state temperature distribution throughout the plate for different plate speeds.

and

$$FF(Re_j) = 2 Re_j^{1/2} \left( 1 + \frac{Re_j^{0.55}}{200} \right)^{0.50} \quad (11)$$

In the above equation,

$$Re_j = \frac{u_j d_j}{\nu} \quad (12)$$

$$Nu = \frac{h_j d_j}{k_f}$$

$Re_j$  = Reynolds number based on nozzle diameter

$Nu$  = Nusselt number based on nozzle diameter

In the above equation,  $\nu$  is the kinematic viscosity,  $h_j$  the average heat transfer coefficient, and  $k_f$  is the thermal conductivity of the coolant fluid. The correlation given in Eq. (9) is valid in the range of

$$2,000 \leq Re_j \leq 400,000$$

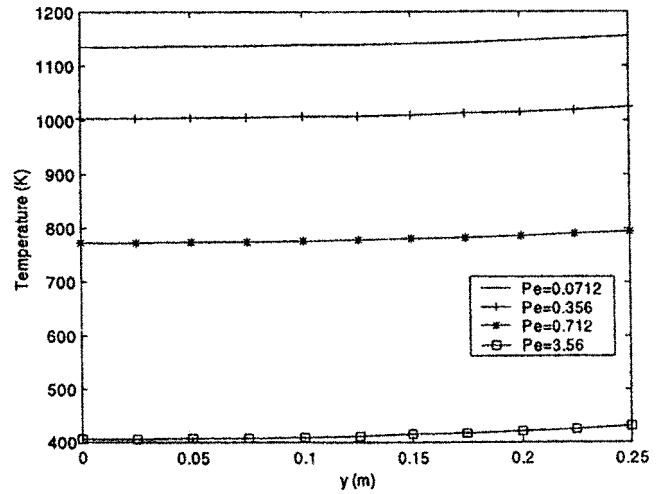
$$2.5 \leq \frac{w_j}{d_j} \leq 7.5 \quad (13)$$

$$2 \leq \frac{Snp_j}{d_j} \leq 12$$

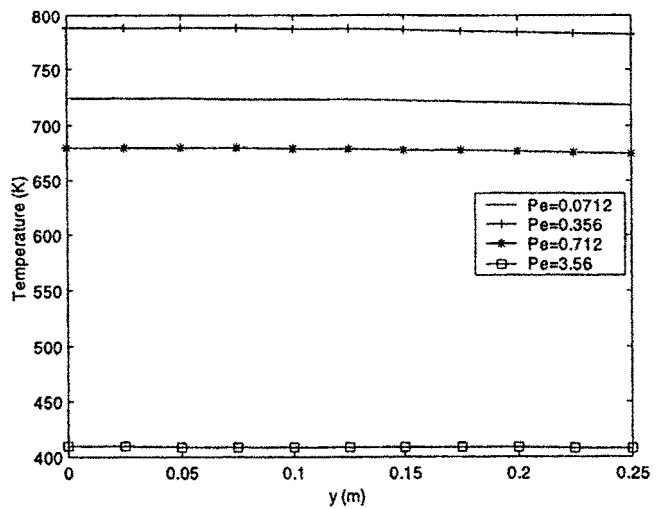
### NUMERICAL SETUP

The numerical analysis is based on finite-difference approximations. The alternating direction implicit (ADI) method is used to carry out the solution for the two-dimensional unsteady heat conduction equation for the moving plate. An analytical solution for the two-dimensional unsteady conduction equation, without the presence of the convective term in the axial direction, can be obtained based on the method of separation of variables [13]. Figure 2 shows excellent agreement between this analytical solution and the numerical results.

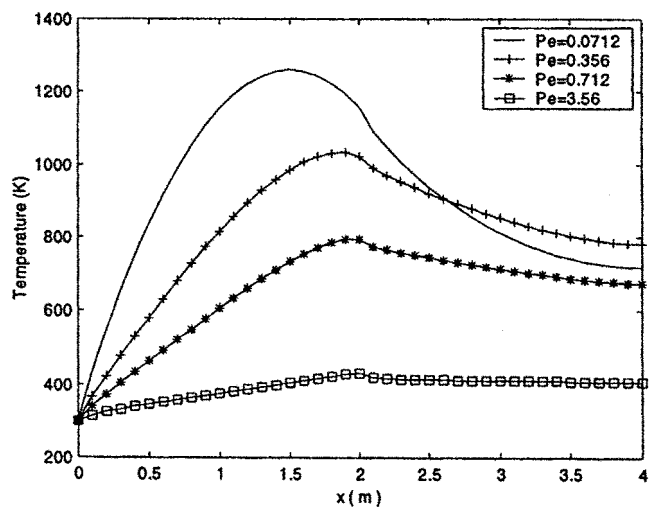
Choudhary and Jaluria [14] have obtained an analytical solution for the two-dimensional unsteady heat conduction equation, with the presence of the convective term in the axial direction and a uniform boundary condition, by employing the coordinate transformation. The final solution is obtained by superposition of both “pseudo-steady” and “pseudo-transient” parts. Figure 3 shows very good agreement between this analytical solution and the numerical results. This analytical solution cannot be used in the present investigation, due to limits imposed by linearity and uniformity of boundary conditions.



(a)



(b)



(c)

**Figure 7** (a) Transverse temperature distribution at the end of the heating section, (b) transverse temperature distribution at the end of the cooling section, and (c) axial temperature distribution at the top surface, for different plate speeds.

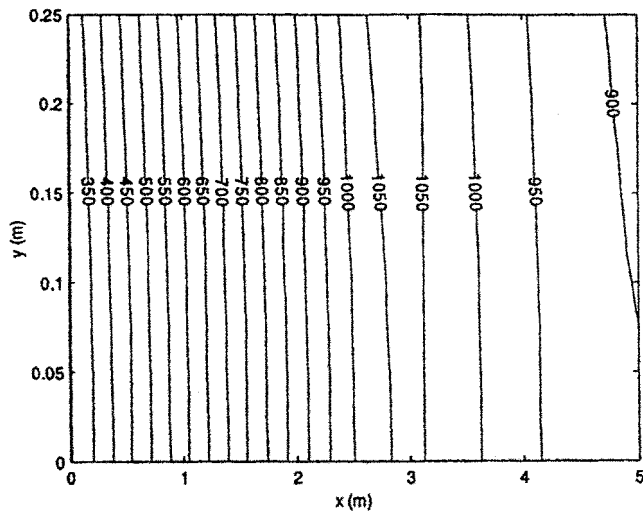
## DISCUSSION OF RESULTS

A parametric study is employed to investigate the effects of various parameters on the temperature distribution and the uniformity of isotherms across the thickness of the metallic plate. The pertinent parameters are heating and cooling lengths, speed of the plate, speed of the cooling fluid, distance from the impinging jet to the plate, and impinging jet diameter. Properties are evaluated at the mean temperature. The property variation is not expected to have a significant effect on the results. The objective of the present work is to produce a more uniform temperature distribution across the plate. This is important because if the top portion is hotter than the bottom surface of the plate or vice versa, the mechanical properties of the metal will be different at the top surface relative to the bottom surface. Therefore, uniform mechanical properties across

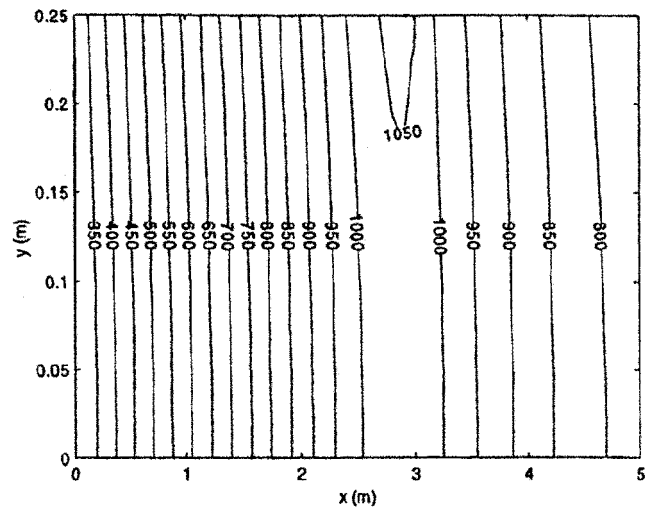
the thickness of the metallic plate cannot be achieved. As such, the uniform temperature across the thickness of the plate is important for heat treatment processes. These pertinent parameters are then designed to control the temperature distribution at the ends of both heating and cooling sections, optimize both heating and cooling lengths, and obtain a uniform temperature distribution across the thickness of the metallic plate. Aluminum is used as plate material, and air is considered as the coolant fluid in this analysis. The gravitational effect is negligible for air, so it is ignored. As a result, symmetric boundary conditions can be assumed for the current analysis.

### Effect of Heating Length

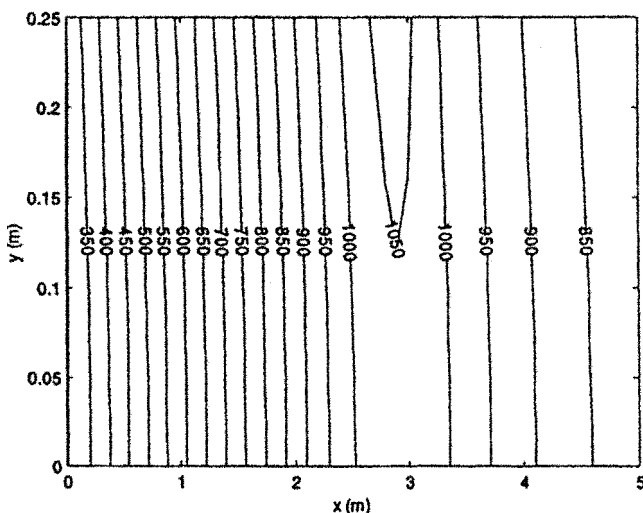
The effect of variations in the heating length is significant on the temperature values and in creating a



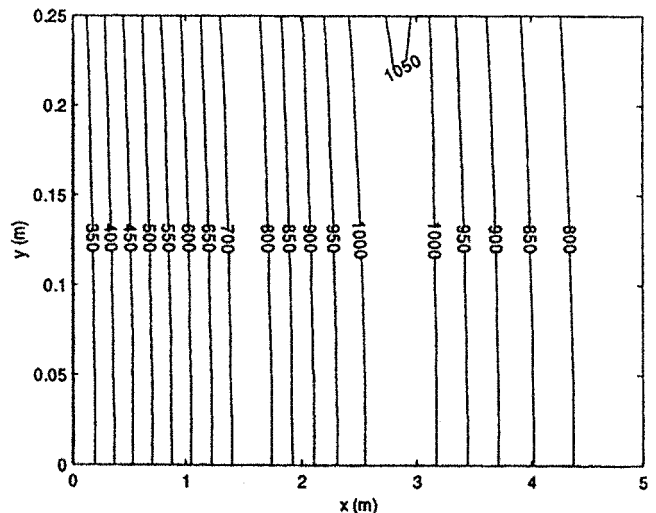
(a)  $Re_1 = 114,000, t = 5.167 \text{ h}$



(c)  $Re_1 = 266,667, t = 4.897 \text{ h}$



(b)  $Re_1 = 200,000, t = 5.005 \text{ h}$



(d)  $Re_1 = 333,333, t = 4.806 \text{ h}$

**Figure 8** Steady-state temperature distribution throughout the plate for different impinging jet speeds.

more uniform distribution across the heating section, as shown in Figures 4 and 5. An increase in the heating length causes an increase in the time it takes to reach steady-state conditions, which in turn increases the overall temperature across the thickness of the plate. An increase in the heating length also causes isotherms to become more uniform across the heating section, as shown in Figures 4a–4d. The temperature distribution is not uniform at the transition stage from heating to cooling sections (Figures 4a–4c), due to the rapid change in temperature at the transition point. These nonuniform distributions tend to decrease with an increase in the heating length, as shown in Figure 4d.

As seen in Figure 5a, the transverse temperature distribution at the end of the heating section becomes more uniform, while the overall temperature increases with an increase in the heating length. The overall transverse temperature at the end of the cooling section increases with an increase in the heating length due to the increase in the heating time, as shown in Figure 5b. Figure 5c clearly illustrates that an increase in the heating length causes an increase in the overall axial temperature distribution at the top surface of the plate.

### Effect of Speed of the Plate

A decrease in the speed of the plate has a significant effect on the temperature values and formation of a more uniform temperature distribution across the thickness of the plate, as shown in Figures 6 and 7. Higher plate speeds lead to a nonuniform distribution, as shown in Figures 6b–6d. The top portion of the plate becomes hotter (cooler) than the bottom portion when the plate is being heated (cooled) at higher plate speeds, thus leading to a more nonuniform structure at higher plate speeds. Both heating and cooling end sections undergo a sharper decrease in temperature across the thickness of the plate with an increase in the speed of the plate, as illustrated in Figures 6 and 7.

### Effect of Impinging Speed

As seen in Figures 8 and 9, an increase in the impinging speed causes an increase in the heat transfer coefficient across the impinging jet, which in turn decreases the time it takes to reach steady-state conditions. The increase in the average heat transfer coefficient also causes a decrease in temperature across the thickness of the plate, as illustrated in Figures 8a–8d. Temperature distribution becomes less uniform at the transition stage from heating to cooling sections (Figures 8b–8d), due to the rapid change in temperature at the transition point.

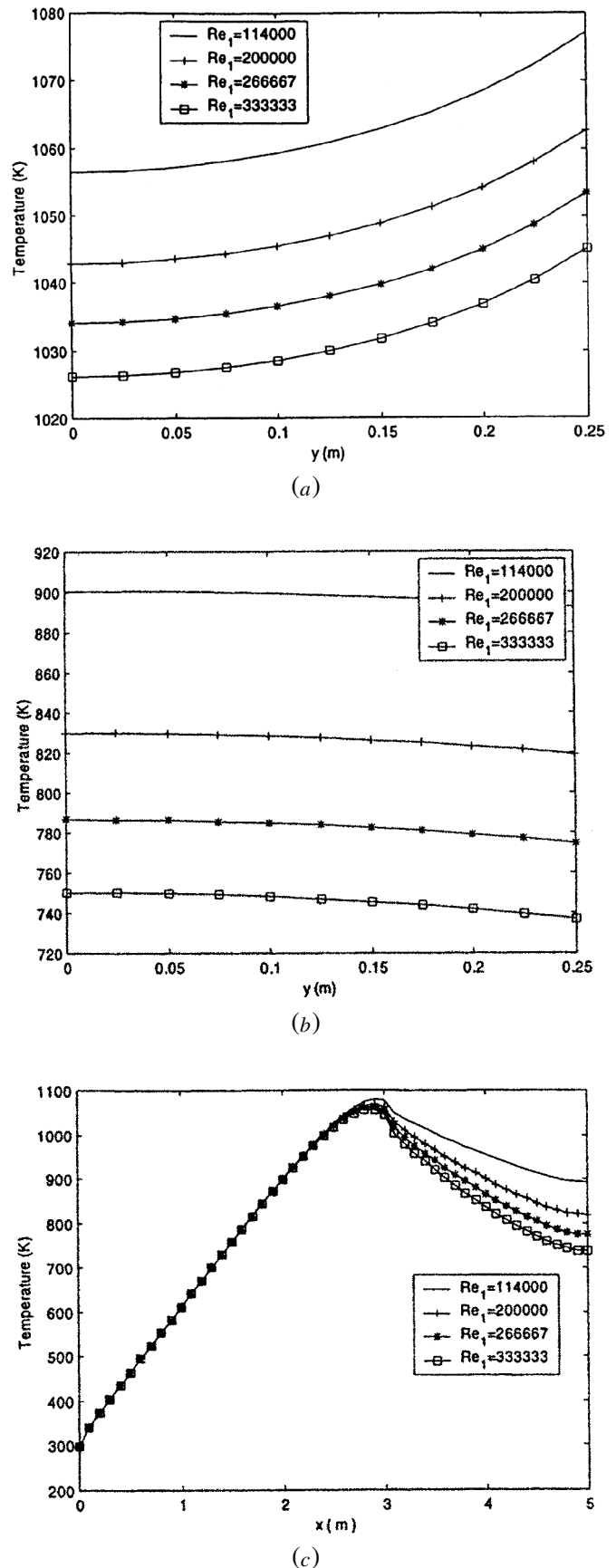


**Figure 9** (a) Transverse temperature distribution at the end of the heating section, (b) transverse temperature distribution at the end of the cooling section, and (c) axial temperature distribution at the top surface, for different coolant speeds.

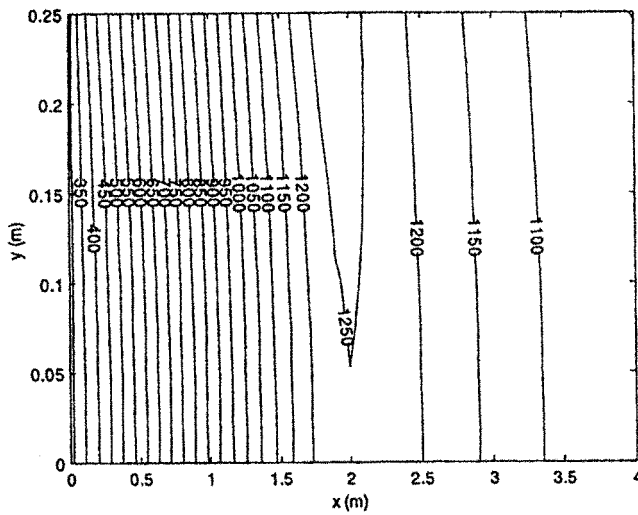
As seen in Figures 9a and 9b, the transverse temperature distribution at both heating and cooling end sections tends to decrease with an increase in the impinging speed, due to the increase in the heat transfer coefficient. The uniformity of the temperature distribution is not affected regardless of variations in the impinging speed, as illustrated in Figures 8 and 9. The axial temperature distribution at the top surface of the plate decreases across the cooling section with an increase in the impinging speed, as shown in Figure 9c.

### Effect of the Distance from the Impinging Jet to the Plate

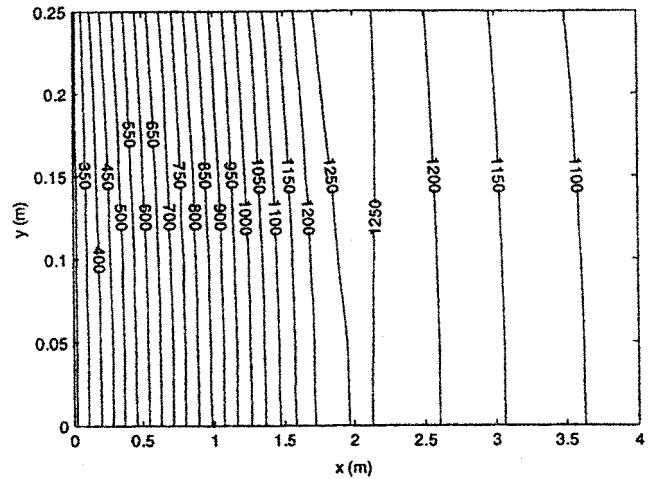
An increase in this distance causes a decrease in the average heat transfer coefficient across the impinging

jet, which in turn increases the time it takes to reach steady-state conditions, as illustrated in Figure 10. The increase in time and the decrease in the average heat transfer coefficient cause an increase in the overall temperature values across the plate, especially in the cooling section, as shown in Figures 10a–10d.

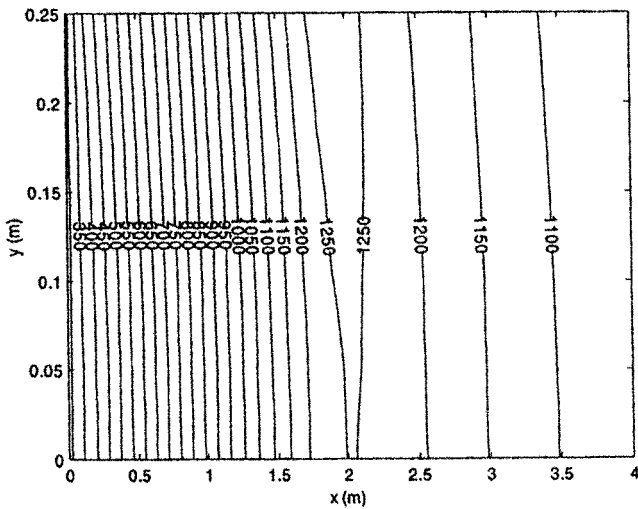
As seen in Figures 11a and 11b, the transverse temperature distribution at both heating and cooling end sections increases with an increase in the distance from the impinging jet to the plate, due to the decrease in the average heat transfer coefficient. The uniformity of the temperature distribution is not affected regardless of variations in this distance, as seen in Figures 10 and 11. The axial temperature distribution at the top surface tends to increase across the cooling section with an increase in this distance, as illustrated in Figure 11c.



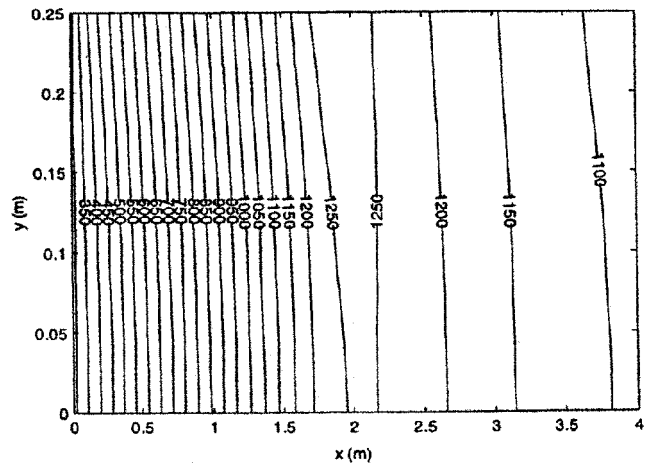
(a)  $\frac{S_{np1}}{d_1} = 3.0, t = 4.169 \text{ h}$



(c)  $\frac{S_{np1}}{d_1} = 9.0, t = 4.675 \text{ h}$

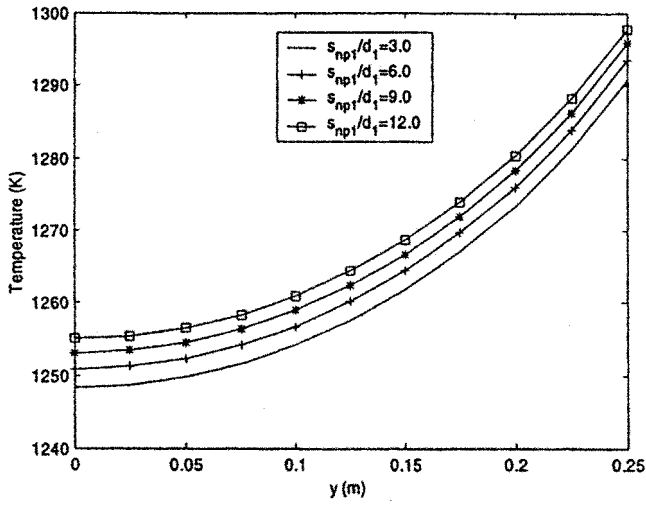


(b)  $\frac{S_{np1}}{d_1} = 6.0, t = 4.646 \text{ h}$

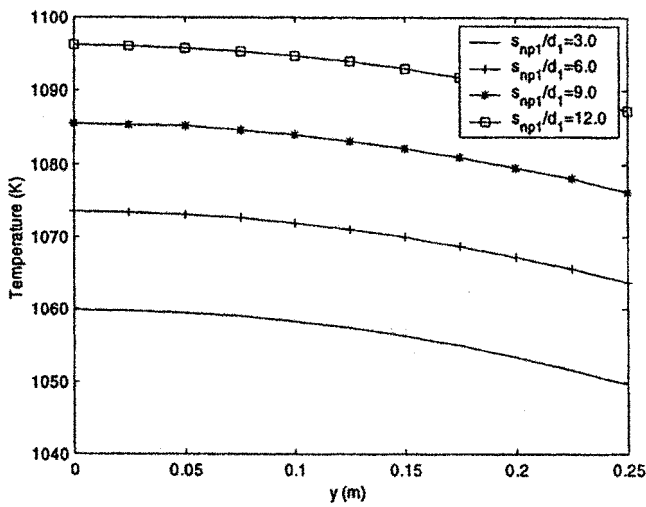


(d)  $\frac{S_{np1}}{d_1} = 12.0, t = 4.700 \text{ h}$

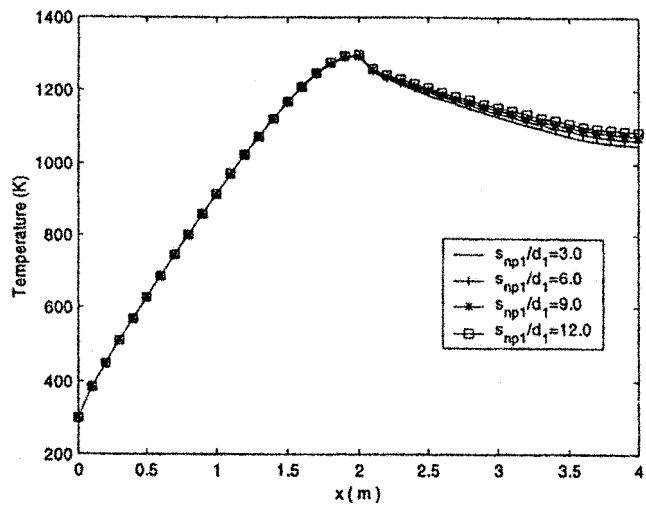
**Figure 10** Steady-state temperature distribution throughout the plate for different  $s_{np}$  distances.



(a)

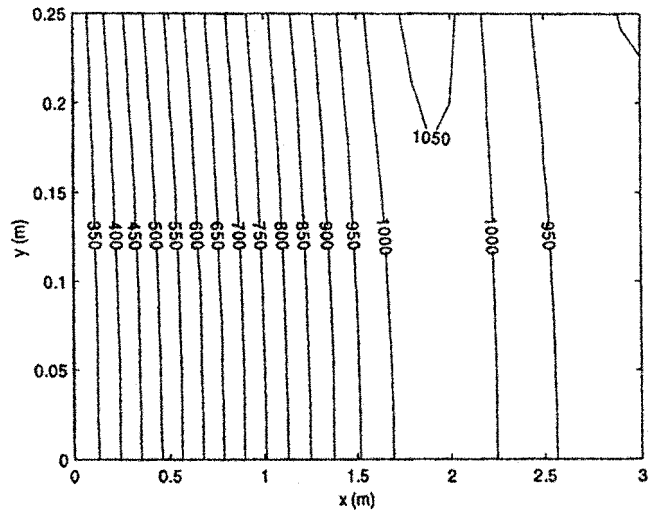


(b)

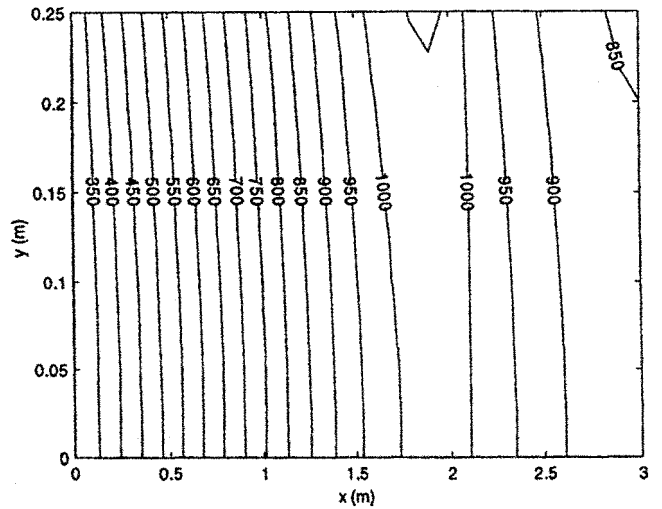


(c)

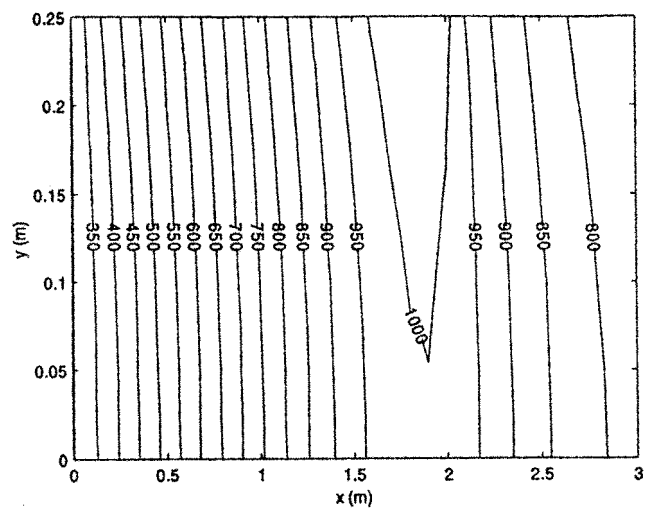
**Figure 11** (a) Transverse temperature distribution at the end of the heating section, (b) transverse temperature distribution at the end of the cooling section, and (c) axial temperature distribution at the top surface, for different  $s_{np}$  distances.



(a)  $\frac{w_1}{d_1} = 2.5$ ,  $\frac{s_{np1}}{d_1} = 2.0$ ,  $Re_1 = 169,765$ ,  $t = 3.648$  h



(b)  $\frac{w_1}{d_1} = 3.33$ ,  $\frac{s_{np1}}{d_1} = 2.67$ ,  $Re_1 = 266,353$ ,  $t = 3.538$  h



(c)  $\frac{w_1}{d_1} = 5.0$ ,  $\frac{s_{np1}}{d_1} = 4.0$ ,  $Re_1 = 339,530$ ,  $t = 3.377$  h

**Figure 12** Steady-state temperature distribution throughout the plate for different nozzle diameters.

### Effect of Impinging Jet Diameter

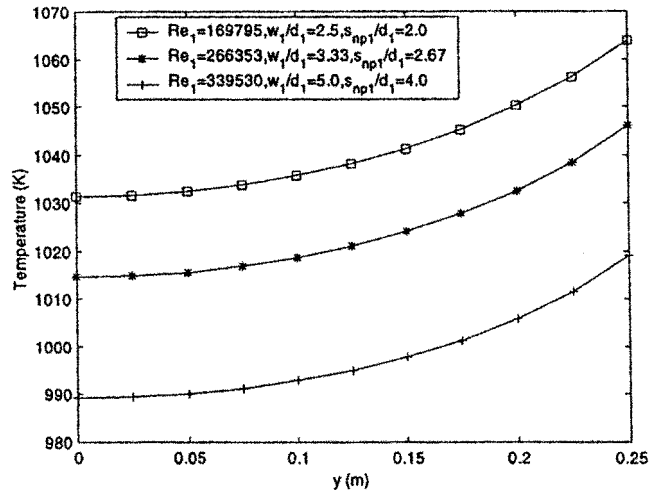
As seen in Figures 12 and 13, a decrease in the impinging jet diameter causes an increase in the average heat transfer coefficient across the impinging jet, which in turn decreases the time it takes to reach steady-state conditions. The increase in the average heat transfer coefficient and the decrease in time lead to decrease in the temperature values across the thickness of the plate, as illustrated in Figures 12a–12d.

As seen in Figures 13a and 13b, the transverse temperature values at both heating and cooling end sections decreases with a decrease in the impinging jet diameter, due to the increase in the average heat transfer coefficient. Varying the impinging jet diameter has no effect on the uniformity of the temperature distribution across the cooling section, as shown in Figures 12 and 13. As seen in Figure 13c, the axial temperature magnitudes at the top surface decreases across the cooling section with a decrease in the impinging jet diameter.

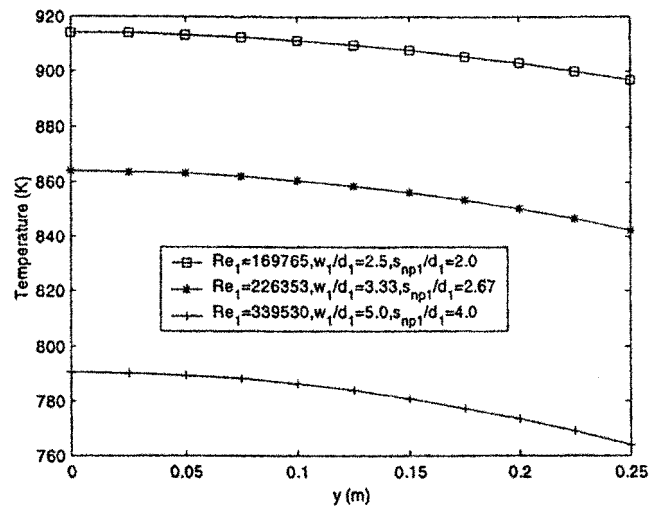
### Effect of Cooling Length

Varying the cooling length has a significant effect on the overall temperature values and the formation of a more uniform temperature distribution across the thickness of the plate, as shown in Figures 14 and 15. It should be noted that a single impinging jet is used in Figures 14a–14c, and multiple impinging jets are utilized in Figure 14d while increasing the cooling length in all cases. As seen in Figures 14a–14c, when using a single jet, an increase in the cooling length causes a decrease in the average heat transfer coefficient across the single impinging jet, which in turn increases the time it takes to reach steady-state conditions. The increase in time causes a small jump in temperature across the heating section, as shown in Figures 14a–14c and 15a. Figures 14a–14c and 15b reveal that the temperature distribution decreases and becomes more uniform across the cooling section with an increase in the cooling length, due to the increase in time and decrease in the average heat transfer coefficient.

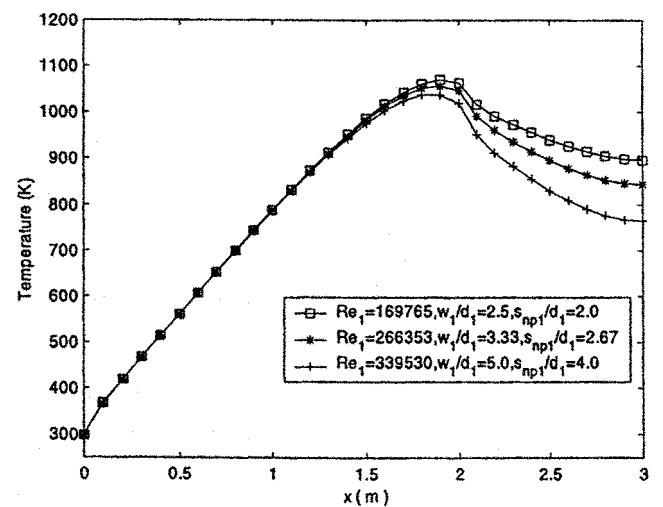
An addition of another impinging jet causes a sharp increase in the average heat transfer coefficient across the multiple impinging jets. As seen in Figures 14d and 15b, multiple impinging jets have a significant impact in reducing the temperature values and generating a more uniform temperature distribution across the cooling section because of the rapid increase in the heat transfer coefficient. The axial temperature distribution at the top surface tends to decrease across the cooling section with an increase in the cooling length, as illustrated in Figure 15c.



(a)

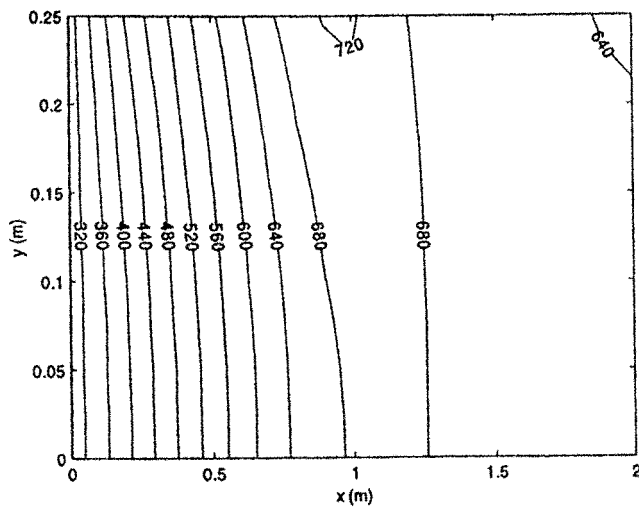


(b)

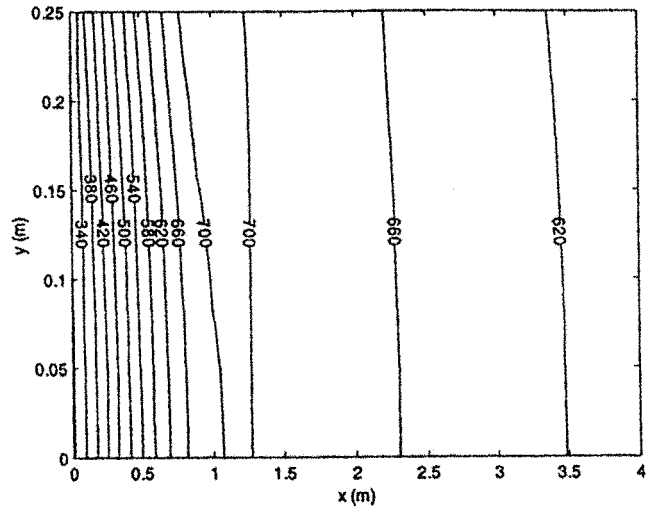


(c)

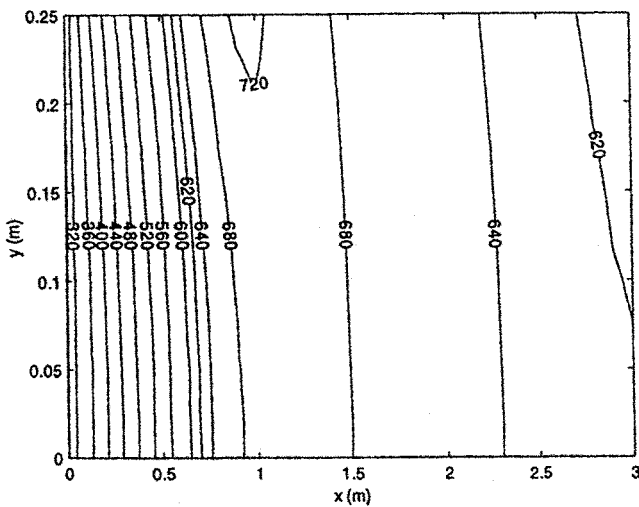
**Figure 13** (a) Transverse temperature distribution at the end of the heating section, (b) transverse temperature distribution at the end of the cooling section, and (c) axial temperature distribution at the top surface, for different nozzle diameters.



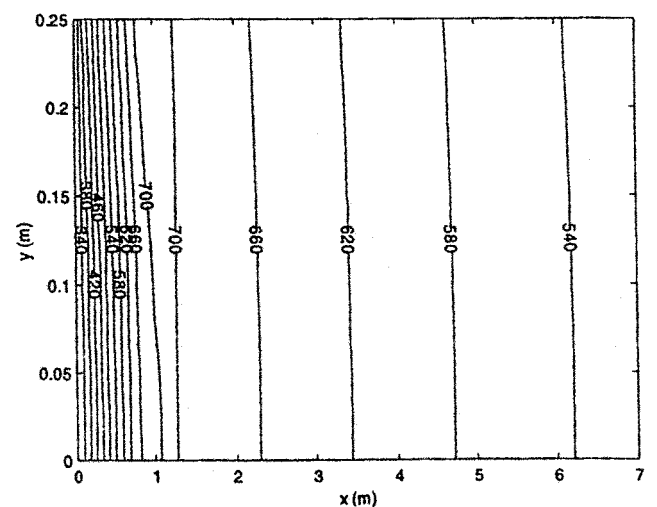
(a)  $K = 1, l_{c1} = 1.0 \text{ m}, Re_1 = 114,000,$   
 $\frac{w_1}{d_1} = 2.5, \frac{S_{np1}}{d_1} = 2.0, t = 2.575 \text{ h}$



(c)  $K = 1, l_{c1} = 3.0 \text{ m}, Re_1 = 114,000,$   
 $\frac{w_1}{d_1} = 7.5, \frac{S_{np1}}{d_1} = 2.0, t = 3.492 \text{ h}$



(b)  $K = 1, l_{c1} = 2.0 \text{ m}, Re_1 = 114,000,$   
 $\frac{w_1}{d_1} = 5.0, \frac{S_{np1}}{d_1} = 2.0, t = 3.492 \text{ h}$



(d)  $K = 2, l_{c1} = 3.0 \text{ m}, l_{c2} = 3.0 \text{ m}, Re_1 = Re_2 = 114,000,$   
 $\frac{w_{1-2}}{d_{1-2}} = 7.5, \frac{S_{np1-2}}{d_{1-2}} = 2.0, t = 6.204 \text{ h}$

**Figure 14** Steady-state temperature distribution throughout the plate for different cooling lengths.

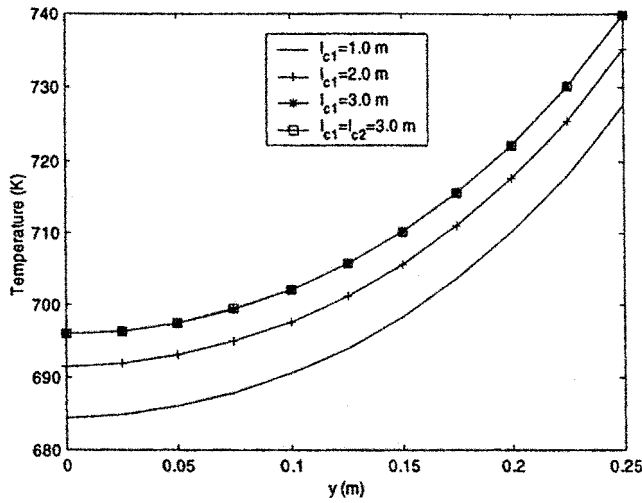
### Optimization Design

The parameters that will produce a uniform temperature distribution within the plate are given in Table 1. These have been obtained for nominal operating temperatures of 1,500 K for heating and 300 K for cooling. From the obtained range of parameters, hardening and

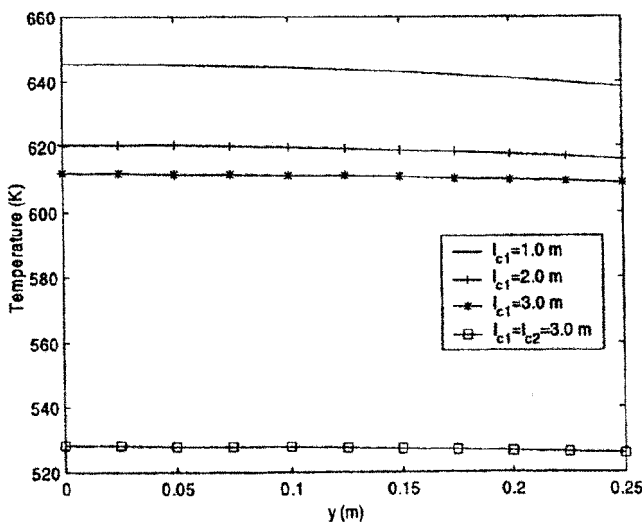
tempering heat treatment processes for the aluminum plate are achieved. Typical heating temperature values related to hardening and tempering heat treatment processes are taken from Kamenichny [15]. Table 1 presents the range of parameters which will result in a uniform temperature at the end of the heating and cooling sections as well as production of the temperature

**Table 1** Range of parameters which result in a uniform temperature distribution within the plate

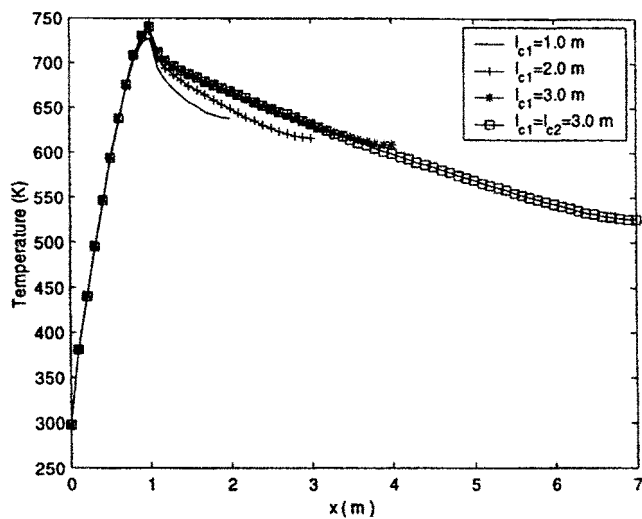
$l_h(m)$	$K$	$l_{c_j}(m)$	$Re_j$	$w_j/d_j$	$s_{npj}/d_j$	Pe
$2 \leq l_h \leq 9$	5	$2 \leq l_{c1} \leq 3$	$2,000 \leq Re_1 \leq 160,000$	$5.0 \leq w_1/d_1 \leq 7.5$	$2.0 \leq s_{np1}/d_1 \leq 12.0$	$0 \leq Pe \leq 0.570$
		$1 \leq l_{c2} \leq 3$	$2,000 \leq Re_2 \leq 400,000$	$2.5 \leq w_2/d_2 \leq 7.5$	$2.0 \leq s_{np2}/d_2 \leq 12.0$	
		$1 \leq l_{c3} \leq 3$	$2,000 \leq Re_3 \leq 400,000$	$2.5 \leq w_3/d_3 \leq 7.5$	$2.0 \leq s_{np3}/d_3 \leq 12.0$	
		$1 \leq l_{c4} \leq 3$	$2,000 \leq Re_4 \leq 400,000$	$2.5 \leq w_4/d_4 \leq 7.5$	$2.0 \leq s_{np4}/d_4 \leq 12.0$	
		$1 \leq l_{c5} \leq 3$	$2,000 \leq Re_5 \leq 400,000$	$2.5 \leq w_5/d_5 \leq 7.5$	$2.0 \leq s_{np5}/d_5 \leq 12.0$	



(a)

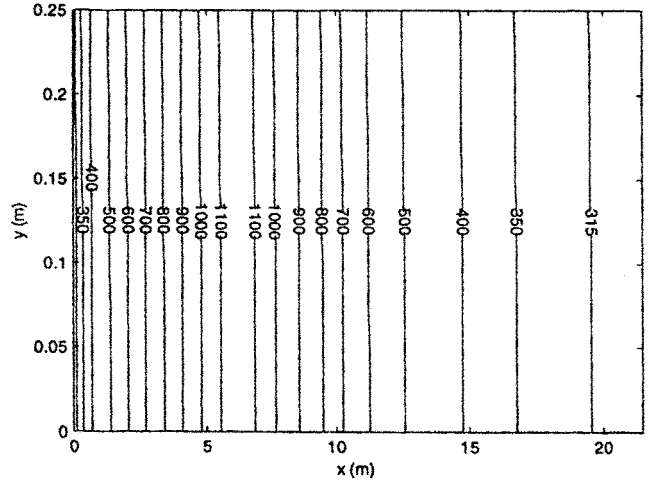


(b)

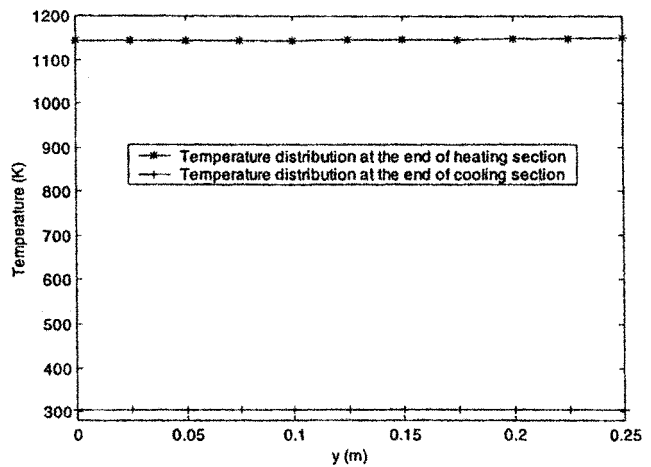


(c)

**Figure 15** (a) Transverse temperature distribution at the end of the heating section, (b) transverse temperature distribution at the end of the cooling section, and (c) axial temperature distribution at the top surface, for different cooling lengths.



(a)



(b)

**Figure 16** (a) Steady-state temperature distribution throughout the plate. (b) Transverse temperature distribution at the end of both heating and cooling lengths in case of hardening, where  $t = 11.695$  h,  $l_h = 6.5$  m,  $K = 4$ ,  $l_{c1 \rightarrow 4} = 3.0$  m,  $Re_1 = 160,000$ ,  $Re_{2 \rightarrow 4} = 400,000$ ,  $w_{1 \rightarrow 4}/d_{1 \rightarrow 4} = 7.5$ ,  $s_{np1 \rightarrow 4}/d_{1 \rightarrow 4} = 2.5$ ,  $q_s = 20,000$  W/m<sup>2</sup>,  $Pe = 0.570$ .

magnitudes required for hardening and tempering processes. As seen in Figures 16 and 17, the use of the optimized parameters, given in Table 1, such as the length scales for the heating and cooling sections, fulfills the objective of the present work: producing a more uniform temperature distribution and controlling the transverse temperature values at both heating and cooling end sections. This information on temperature distribution will be useful in the design of heat treatment processes. For example, the optimized values can be used to alternate the mechanical properties of the aluminum plate for hardening and tempering heat treatments.

## CONCLUSION

A parametric study is employed to investigate various quantities that affect the temperature distribution

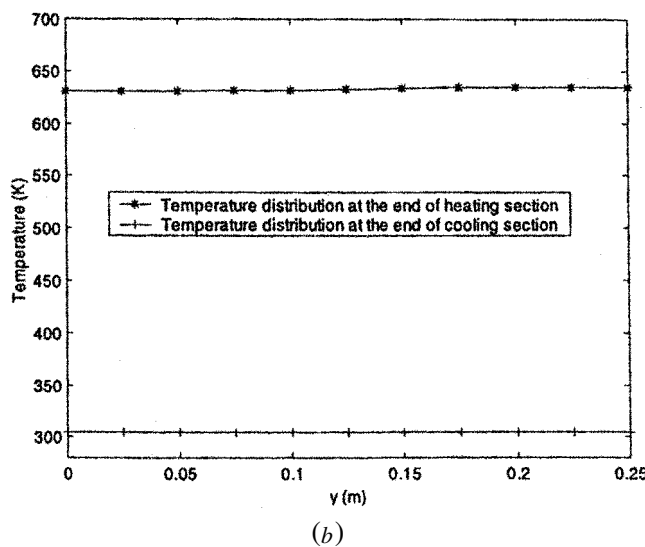
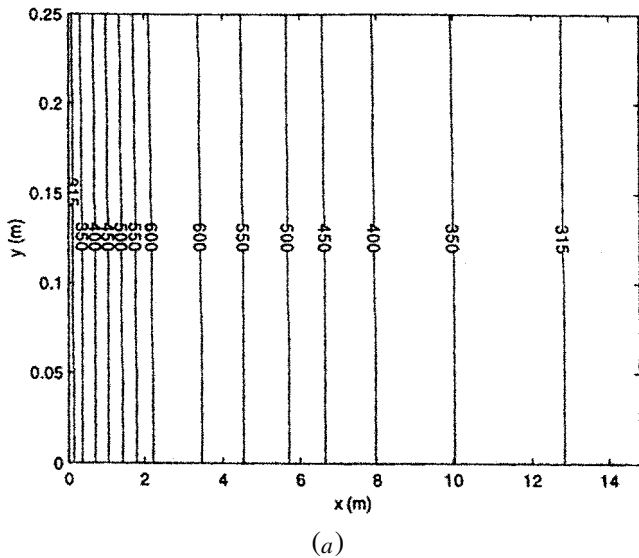


**Figure 17** (a) Steady-state temperature distribution throughout the plate. (b) Transverse temperature distribution at the end of both heating and cooling lengths in case of tempering, where,  $t = 8.716$  h,  $l_h = 2.8$  m,  $K = 4$ ,  $l_{c1 \rightarrow 4} = 3.0$  m,  $Re_1 = 160,000$ ,  $Re_{2 \rightarrow 4} = 400,000$ ,  $w_{1 \rightarrow 4}/d_{1 \rightarrow 4} = 7.5$ ,  $s_{npj1 \rightarrow 4}/d_{1 \rightarrow 4} = 2.5$ ,  $q_s = 20,000$  W/m<sup>2</sup>,  $Pe = 0.570$ .

and uniformity of isotherms in the heat treatment of metallic plates. The pertinent parameters are heating and cooling lengths, the distance from the impinging jet to the plate, the speed of the coolant fluid, the diameter of the impinging jet, and the speed of the plate. These pertinent parameters are optimized for both hardening and tempering heat treatments for a metallic plate. The main conclusions of this investigation are as follows:

1. The temperature distribution increases and becomes more uniform across the heating section with an increase in the heating length.
2. Nonuniformity increases with an increase in the plate speed.

3. The uniformity across the cooling section is not affected by variations in the distance from the impinging jet to the plate, the speed of the coolant fluid, or the impinging jet diameter.
4. The overall temperature values decrease across the cooling section with a decrease in the diameter of the impinging jet.
5. The overall temperature values increase across the cooling section with an increase in the distance from the impinging jet to the plate.
6. The temperature values decrease across the cooling section with an increase in the impinging speed.
7. The temperature values across the cooling section decrease and become more uniform with an increase in the cooling length. The addition of another impinging jet has a significant impact on reducing the temperature values across the cooling section and creating a more uniform temperature distribution.

## NOMENCLATURE

$b$	thickness of the plate, m
$Bi$	Biot number ( $=h_j/k_p$ )
$d_j$	diameter of impinging jet, cm
$F$	shape factor
$FF$	Reynolds function for the impinging jet
$G$	geometric function for the impinging jet
$h$	heat transfer coefficient, W/m <sup>2</sup> K
$h_j$	average heat transfer coefficient across the impinging jet, W/m <sup>2</sup> K
$K$	number of impinging jet
$k_f$	thermal conductivity of the fluid, W/m K
$k_p$	thermal conductivity of the plate, W/m K
$l_{cj}$	cooling length, m
$l_h$	heating length, m
$Nu$	Nusselt number ( $=h_j d_j/k_f$ )
$Pe$	Peclet number ( $=u_p r/\alpha$ )
$Pr$	Prandtl number
$q_s$	constant heat flux, W/m <sup>2</sup>
$Re_j$	Reynolds number ( $=u_j d_j/\nu$ )
$s_{npj}$	distance from the plate to the impinging jet, m
$t$	time, h
$T$	temperature, °C or K
$T_{ENT}$	entrance temperature, K
$T_e$	ambient temperature, K
$T_i$	initial temperature condition, K
$T_w$	temperature of the coolant fluid, K
$u_j$	speed of the coolant fluid, m/s
$u_p$	speed of the plate, m/s
$w_j$	radius of the cooling length, m
$x$	axial coordinate distance, m
$X$	dimensionless axial coordinate distance, ( $=x/r$ )

$y$	transverse coordinate distance, m
$Y$	dimensionless transverse coordinate distance, ( $=y/r$ )
$\alpha$	thermal diffusivity, $m^2/s$
$\theta$	dimensionless temperature [ $=(T - T_\infty)/(T_i - T_\infty)$ ]
$\varepsilon$	emissivity
$\nu$	kinematic viscosity, $m^2/s$
$\sigma$	Stefan-Boltzman constant, $W/m^2 K^4$

### Subscripts

$c$	cooling length
$f$	fluid
$h$	heating length
$j$	impinging jet

### REFERENCES

- [1] Niebel, B. W., Draper, A. B., and Wysk, R. A., *Modern Manufacturing Process Engineering*, pp. 56-60, McGraw-Hill, New York, 1989.
- [2] Winning, J., *Heat Treatment of Metals*, pp. 7-10, Chemical Publishing Co., New York, 1943.
- [3] Kang, B. H., Jaluria, Y., and Karwe, M. V., Numerical Simulation of Conjugate Transport from a Continues Moving Plate in Materials Processing, *Numer. Heat Transfer A*, vol. 19, pp. 151-176, 1991.
- [4] Jaluria, Y., and Singh, A. P., Temperature Distribution in Moving Materials Subjected to Surface Energy Transfer, *Comput. Math. Appl. Mech. Eng.*, vol. 41, pp. 145-157, 1983.
- [5] Karwe, M. V., and Jaluria, Y., Thermal Transport from a Heated Moving Surface, *J. Heat Mass Transfer*, vol. 108, no. 4, pp. 728-733, 1986.
- [6] Karwe, M. V., and Jaluria, Y., Fluid Flow and Mixed Convection Transport from a Moving Plate in Rolling and Extrusion Processes, *J. Heat Transfer*, vol. 110, pp. 655-661, 1988.
- [7] Karwe, M. V., and Jaluria, Y., Numerical Simulation of Thermal Transport Associated with a Continuously Moving Flat Sheet in Materials Processing, *J. Heat Transfer*, vol. 113, pp. 612-619, 1991.
- [8] Kang, B. H., and Jaluria, Y., Numerical Study of the Fluid Flow and Heat Transfer Due to a Heated Plate Moving in a Uniform Forced Flow, *Numer. Heat Transfer*, vol. 22, pp. 143-165, 1992.
- [9] Chen, J., Wang, T., and Zumbrennen, D. A., Numerical Analysis of Convective Heat Transfer from a Moving Plate Cooled by an Array of Submerged Planner Jets, *HTD-vol. 162*, pp. 25-34, 1991.
- [10] Taga, M., Ochi, T., and Akagawa, K., Cooling of a Hot Moving Plate by an Impinging Water Jet, *Proc. ASME-JSME Joint Cong.*, Honolulu, HI, vol. 1, pp. 183-189, 1983.

- [11] Lee, D. Y., and Vafai, K., Comparative Analysis of Jet Impingement and Microchannel Cooling for High Flux Applications, *Int. J. Heat Mass Transfer*, vol. 42, no. 9, pp. 1555-1568, 1999.
- [12] Martin, H., Heat and Mass Transfer between Impinging Gas Jets and Solid Surfaces, in *Advances in Heat Transfer*, vol. 8, pp. 1-60, Academic Press, New York, 1977.
- [13] Kakac, S., and Yener, Y., *Heat Conduction*, 3d ed., pp. 201-203, Taylor & Francis, Washington, DC, 1993.
- [14] Choudhury, S. R., and Jaluria, Y., Analytical Solution for the Transient Temperature Distribution in a Moving Rod or Plate of Finite Length with Surface Heat Transfer, *Int. J. Heat Mass Transfer*, vol. 37, pp. 1193-1205, 1994.
- [15] Kamenichny, I., *A Short Handbook of Heat Treatment*, pp. 205-210, Pervy Rizhsky Pereulok, Moscow, 1963.



**Ahmad A. Ali** earned a B.S. in Mechanical Engineering from Ohio Northern University in 1995. He has worked as a Research Assistant at Kuwait Institute for Scientific Research for the past 5 years. He received his M.S. in Mechanical Engineering from the Ohio State University in 1999. He is currently involved in Ph.D. studies at the Ohio State University. His areas of interest are

computational fluid dynamics and heat transfer, and assessment of different types of thermal systems.



**Kambiz Vafai** received his B.S. in Mechanical Engineering from the University of Minnesota in Minneapolis in 1975. He received his M.S. (1977) and Ph.D. (1980) in Mechanical Engineering from the University of California at Berkeley. After spending a year as a Postdoctoral Fellow at Harvard University, he joined The Ohio State University in the Department of Mechanical Engineering as an Assistant Professor in 1981. He was promoted to the rank of Professor in 1991. Dr. Vafai has authored numerous journal publications and book chapters and has been an invited Visiting Professor at the Technical University of Munich in Germany, University of Bordeaux and Paul Sabatier University in France, and Technical University of Naples in Italy.

He has done extensive research work for a variety of industrial companies and governmental agencies and has given numerous national and international invited talks and seminars. Dr. Vafai, is a Fellow of the American Society of Mechanical Engineers and Associate Fellow of the American Institute of Aeronautics and Astronautics. Dr. Vafai is the Editor in Chief of the *Journal of Porous Media* and is on the Board of Editors for *Experimental Heat Transfer*. He is also on the Editorial Advisory Board of the *International Journal of Heat and Mass Transfer* and has been an Associate Editor of the *ASME Journal of Heat Transfer* and on the Editorial Board of the *International Journal of Heat and Fluid Flow*. Dr. Vafai has done extensive investigations in the areas of transport through porous media and multiphase transport, natural convection in complex configurations, analysis and modeling of flat-shaped heat pipes, analysis of porous insulations, high-energy storage and recovery, electronic cooling, and free surface flows.